Original Article

miR-613 suppresses ischemia-reperfusion-induced cardiomyocyte apoptosis by targeting the programmed cell death 10 gene

Zhenhua Wu[1], Yujuan Qi[1], Zhigang Guo[2,*], Peijun Li[1], Ding Zhou[3]

[1] *ICU, Departmentof Cardiac Surgery, Tianjin Chest Hospital, Tianjin, China;*
[2] *Department of Cardiac Surgery, Tianjin Chest Hospital, Tianjin, China;*
[3] *TEDA International Cardiovascular Hospital, Tianjin, China.*

Summary   MicroRNAs (miRNAs) are important gene regulators in both biological and pathological processes, including myocardial ischemia/reperfusion (I/R) injury. This study investigated the effect of miR-613 on I/R-induced cardiomyocyte apoptosis and its molecular mechanism of action. Hypoxia/reoxygenation (H/R) significantly increased the release of lactate dehydrogenase (LDH), levels of malondialdehyde (MDA), and cardiomyocyte apoptosis, but these effects were attenuated by an miR-613 mimic. Programmed cell death 10 (PDCD10) was identified as a target gene of miR-613. miR-613 significantly increased the phosphorylation of Akt (p-Akt). An miR-613 mimic lowered the level of expression of pro-apoptotic proteins, C/EBP homologous protein (CHOP), and phosphorylated c-Jun N-terminal kinase (p-JNK), and it up-regulated the expression of the anti-apoptotic protein B-cell lymphoma-2 (Bcl-2). All of these effects were reversed by restoration of PDCD10. Taken together, the current findings indicate that miR-613 inhibits I/R-induced cardiomyocyte apoptosis by targeting PDCD10 by regulating the PI3K/AKT signaling pathway.

Keywords: miRNAs, hypoxia/reoxygenation, C/EBP homologous protein, B-cell lymphoma-2, PI3K/AKT

1. Introduction

Myocardial ischemia/reperfusion (I/R)-induced cardiac injury after myocardial ischemia, cardiac surgery, or cardiac arrest leads to a high mortality rate in humans with coronary heart disease. I/R injury causes local myocardial inflammation and apoptosis, resulting in irreversible damage to the myocardium (*1*). Several mechanisms underlying myocardial I/R injury have been elucidated, including formation of oxygen free radicals, intracellular Ca^{+} overload, neutrophil activation, and vascular endothelium damage (*2*). However, the complete profile of molecular pathways associated with myocardial I/R injury is not yet fully understood.

MicroRNAs (miRNAs) are highly conserved, small, noncoding RNAs that can regulate cell proliferation, migration, differentiation, apoptosis, and immune response at the post-transcriptional level. Recent studies have reported that miRNAs play an important role in myocardial I/R injury and may become potential targets for diagnosis and therapy. As an example, miR-93 inhibits I/R-induced cardiomyocyte apoptosis by targeting PTEN (*3*). miR-17 attenuates apoptosome formation and cardiomyocyte apoptosis by regulating apoptotic protease activation factor 1 (*4*).

Mounting evidence has indicated that miR-613 is involved in multiple processes, including tumorigenesis, metastasis, lipogenesis, and lipoprotein metabolism (*5-8*). However, the role of miR-613 in myocardial I/R injury has not been examined. The current study found that miR-613 suppresses cardiomyocyte apoptosis induced by hypoxia/reoxygenation (H/R) in H9c2 cells. PDCD10 was identified as a direct target of miR-613. This study also examined the level of expression of p-Akt and downstream signaling proteins such as CHOP, p-JNK, and Bcl-2. miR-613 was found to affect I/R-induced cardiomyocyte apoptosis by regulating the

PI3K/Akt signaling pathway. Together, these findings reveal part of the miR-613/PDCD10 /PI3K/Akt pathway that mediates I/R-induced cardiomyocyte apoptosis.

2. Materials and Methods

2.1. *Cell culture and miRNA transfection*

H9c2 cells were cultured in DMEM containing 10% fetal bovine serum (FBS) at 37°C with 5% CO_2. An miR-613 mimic, an miR-613 inhibitor, and a corresponding control (miR-NC) were synthesized by GenePharma (Shanghai, China). H9c2 cells were cultured in six-well plates and transfected with an miR-613 mimic, an miR-613 inhibitor, or miR-NC using Lipofectamine 2000 reagent according to the manufacturer's instructions (Invitrogen, USA).

2.2. *Construction of vectors*

The EGFP coding region from the pEGFP-N2 vector was subcloned into pcDNA3. The 3'-UTR of wild-type or mutant-type PDCD10 was then cloned into a pcDNA3-EGFP vector. A PDCD10 expression plasmid, pcDNA3-PDCD10, was constructed by cloning the coding sequence of PDCD10 into a pcDNA3 vector.

2.3. *Detection of LDH and MDA*

Lactate dehydrogenase (LDH) and malondialdehyde (MDA) commercial kits were purchased from Sangon Biotech (Shanghai, China). LDH and MDA were measured according to the manufacturer's instructions.

2.4. *In vitro hypoxia/reoxygenation (H/R) model*

Cardiomyocytes were perfused in normal Hank's solution with a gas mixture of 95% O_2-5% CO_2 at 37°C, pH 7.4. To simulate an ischemic environment, cardiomyocytes were perfused in Hank's solution at a pH of 7.4 at 37°C without glucose or calcium. Cells were then exposed to a gas mixture of 95% N_2-5% CO_2. To simulate a reperfusion environment, cells were again perfused in normal Hank's solution with a gas mixture of 95% O_2-5% CO_2 at 37°C, pH 7.4 (*9*). Cells in a normoxic environment served as the corresponding control.

2.5. *Analysis of apoptosis*

Cell apoptosis were detected using the Annexing V-FITC/propidium iodide (PI) apoptosis detection kit (BD Biosciences, Shanghai, China). Cells were harvested and collected after centrifugation for 5 to 10 minutes at 2,000 rpm. Cells were then washed with phosphate-buffered saline (PBS) and suspended in 300 µL of Binding Buffer. An Annexin V-FITC solution (5 µL) was added to the cell suspension, which was incubated for 15 min in the dark. Five µL of PI was then added to the suspension.

Cell apoptosis was analyzed with a flow cytometry system (BD Bioscience, Shanghai, China). Healthy living cells are denoted as FITC-/PI- cells, early apoptotic cells are denoted as FITC+/PI- cells, and necrotic and late apoptotic cells are denoted as FITC+/PI+ cells.

2.6. *Reverse transcription-quantitative polymerase chain reaction (RT-qPCR)*

Total RNA and microRNA were extracted using Trizol reagent (Invitrogen) and the mirVana miRNA isolation kit (Ambion, Austin, TX, USA). RNA integrity was verified with agarose gel electrophoresis. cDNA was obtained using the Taqman® RNA reverse transcription kit. cDNA was then subjected to RT-qPCR using SYBR Premix Ex Taq (TaKaRa, Dalian, China) to measure the relative level of miR-613 and PDCD10 mRNA expression. β-actin and U6 served as corresponding controls. The relative level of gene expression was analyzed using the $2^{-\Delta\Delta Ct}$ method.

2.7. *Western blot analysis*

Cell protein was extracted with the RIPA lysis buffer (BLKW Biotechnology, Beijing, China). Equal amounts of protein were separated by sodium dodecyl sulfate-polyacrylamide gel electrophoresis (SDS-PAGE) and then transferred to nitrocellulose membranes. The membranes were blocked with 5% skim milk for 2 h and then incubated with primary antibodies that were purchased from Cell Signaling Technology. The primary antibodies used were as follows: PDCD10 (1:500), p-AKT (1:1,000), glucose-regulated protein (GRP) 78 (1:500), caspase-12 (1:500), CHOP (1:1,000), p-JNK (1:1,000), and Bcl-2 (1:500). Goat anti-rabbit secondary antibody was added and cells were incubated at room temperature for 2 h. Bands were visualized with an enhanced chemiluminescence (ECL) regent (Santa Cruz Biotechnology, CA, USA). Glyceraldehyde phosphate dehydrogenase (GAPDH) served as the internal control.

2.8. *EGFP reporter assay*

Cells were transfected with an miR-613 mimic, an miR-613 inhibitor, or a reporter plasmid carrying a wild-type or mutant PDCD10-3'UTR. Fluorescence intensity was detected with an F-4500 fluorescence spectrophotometer (Hitachi, Tokyo, Japan). An RFP expression vector served as a reporter control. The relative fluorescence intensity of EGFP was determined with respect to the RFP intensity.

2.9. *Statistical analysis*

The statistical software Graphpad 5.0 was used to

analyze data. Data are expressed as the mean ± standard deviation (mean ± S.D.). One-way ANOVA was used to compare differences among groups. A two-tailed Student's *t*-test was used to compare differences between two groups. A p-value of less than 0.05 was considered statistically significant.

3. Results

3.1. *miR-613 was down-regulated in H9c2 cells after H/R*

To explore the potential role of miR-613 in myocardial I/R injury, the expression of miR-613 was detected in H9c2 cells after 10 h in a hypoxic environment and 2 h of deoxygenation. Data indicated that miR-613 expression was reduced by almost 43% in H9c2 cells after H/R treatment compared to cells under normoxia. This result suggested that miR-613 may play a role in the H/R injury of H9c2 cells (Figure 1).

3.2. *MiR-613 alleviated H/R-induced cardiomyocyte injury*

Since the release of LDH is an important sign of cell injury, the release of LDH by H9c2 cells was examined. Results indicated that H/R treatment significantly increased the release of LDH. The miR-613 mimic decreased the release of LDH by approximately 49% while the miR-613 inhibitor increased the release of LDH by almost 1.3-fold in response to H/R in H9c2 cells (Figure 2A).

MDA is a key index of membrane lipid peroxidation. Levels of MDA were also measured. As shown in Figure 2B, levels of MDA in cells increased significantly after H/R treatment in comparison to levels in control cells. Similarly, miR-613 decreased an H/R-induced increase in MDA levels by 52% while inhibition of miR-613 increased MDA levels by almost 1.4-fold (Figure 2B).
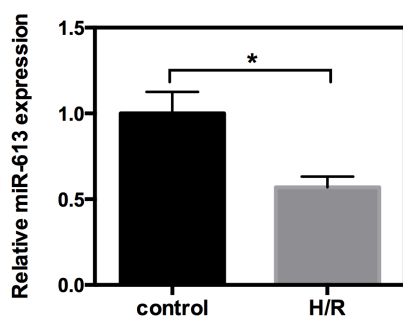
3.3. *miR-613 suppressed H/R-induced cardiomyocyte apoptosis in vitro*

The above results suggested that miR-613 expression decreased in H9c2 cells after H/R, so the question was then whether or not miR-613 protected cardiomyocytes from H/R-induced injury by affecting cell apoptosis. The effect of miR-613 on cardiomyocyte apoptosis was detected using flow cytometry. Data indicated that overexpression of miR-613 significantly reduced the rate of apoptosis during H/R. However, inhibition of miR-613 markedly increased the rate of apoptosis compared to that in cells treated with H/R alone (Figure 3A).

To further explore the potential molecular mechanism of action of miR-613, expression of apoptosis-related proteins such as GRP78, caspase-12, cytochrome c, Bax, and caspase-3 was examined. Results suggested that H/R markedly increased the level of expression of these proteins, but that increase was reversed by miR-613 overexpression. In contrast, inhibition of miR-
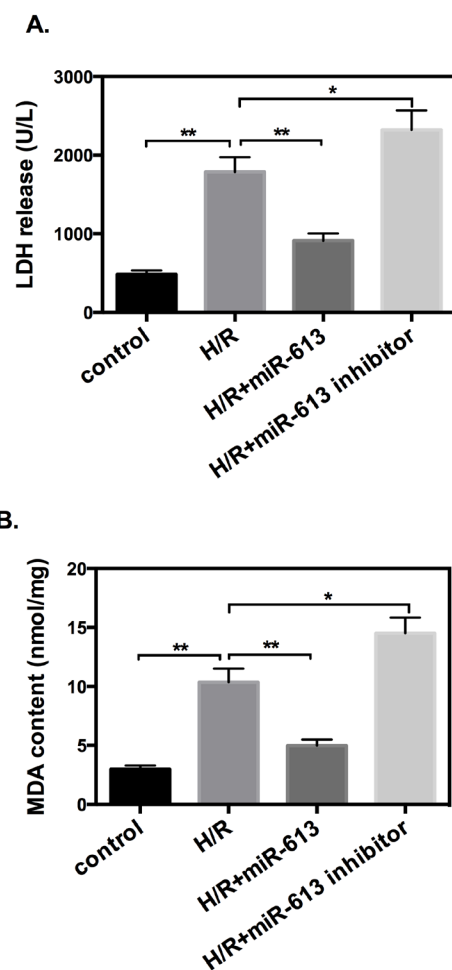
A.

B.

Figure 2. miR-613 alleviated H/R-induced cardiomyocyte injury. (A), Release of LDH. **(B)**, Levels of MDA. *$p < 0.05$, ***p < 0.01$. (*Note*: H/R+miR-613: H9c2 cells were transfected with an miR-613 mimic after H/R treatment; H/R+miR-613 inhibitor: H9c2 cells were transfected with an miR-613 inhibitor after H/R treatment. Data are expressed as the mean ± S.D.)

Figure 1. miR-613 was down-regulated in H9c2 cells after H/R. RT-qPCR was used to detect the expression of miR-613 in H9c2 cells after H/R or under normoxia. Cells under normoxia served as the control group. The level of miR-613 expression in the control group was normalized to 1. U6 served as a loading control. *$p < 0.05$.
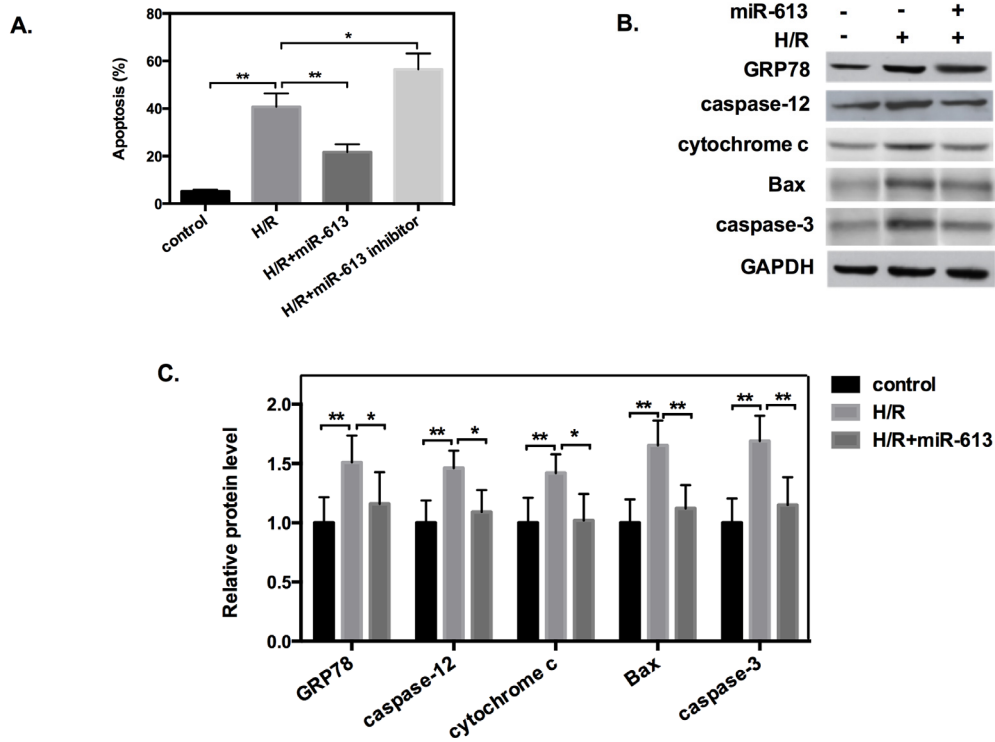
Figure 3. miR-613 suppressed H/R-induced cardiomyocyte apoptosis *in vitro*. (A) The rate of cell apoptosis was detected with an Annexin V/Propidium iodide apoptosis assay after transfection with an miR-613 mimic or inhibitor. **(B)**, Western blot analysis of the level of GRP78, caspase-12, cytochrome c, Bax, and caspase-3 proteins with or without transfection of miR-613 after H/R treatment. Levels of protein expression in the control group were normalized to 1. GAPDH served as the internal control. **(C)**, Statistical analysis of levels of protein expression. The histogram shows the mean ± S.D. for normalized GAPDH. *$p < 0.05$, **$p < 0.01$.
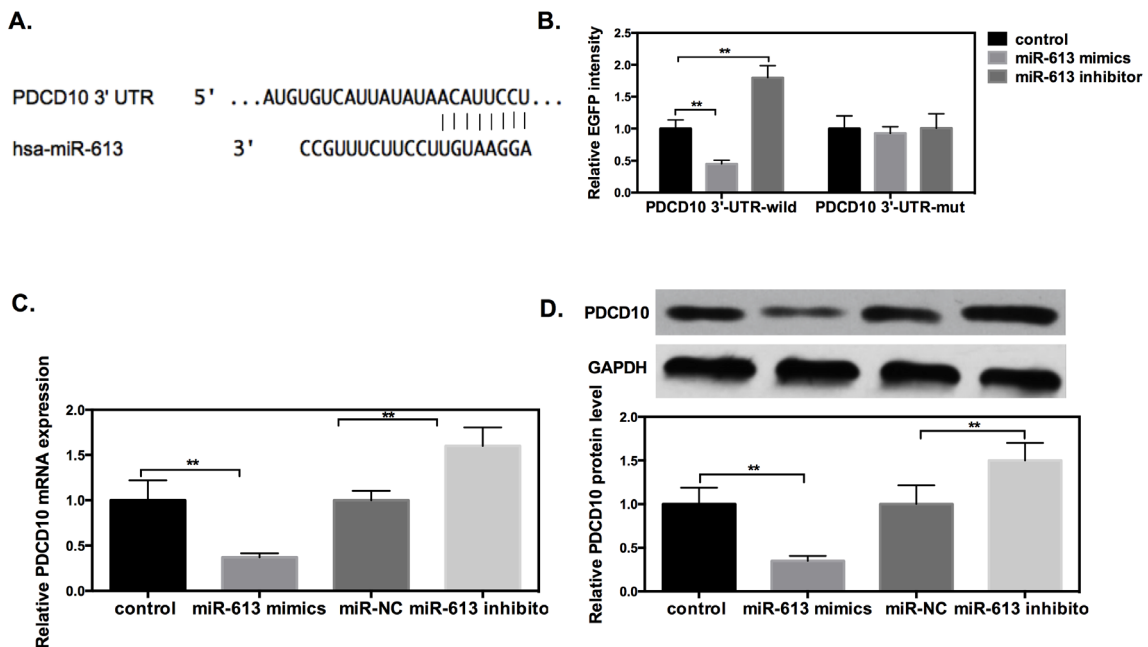

Figure 4. miR-613 directly targeted PDCD10 by binding to its 3'-UTR. (A) The potential binding site for miR-613 in the 3'-UTR of PDCD10 mRNA. **(B)** EGFP reporter analysis was performed to detect relative EGFP activity after a wild-type or mutant-type reporter plasmid was co-transfected with an miR-613 mimic, an miR-613 inhibitor, or miR-NC control in H9c2 cells. Relative EGFP intensity was determined as the ratio to the RFP intensity. **(C)** RT-qPCR was used to detect the level of PDCD10 mRNA in transfected cells. β-actin was used as the corresponding control. **(D)** The level of PDCD10 protein was detected with Western blot analysis in transfected H9c2 cells. Normalization was performed using GAPDH. **$p < 0.01$.

613 significantly increased the level of expression of apoptosis-related proteins (Figure 3B and 3C).

3.4. *miR-613 directly targeted PDCD10 by binding to its 3'-UTR*

miRNAs act by regulating target genes. To investigate the exact mechanism by which miR-613 affects cell apoptosis induced by H/R, TargetScan, miRanda, and PicTar were used to predict the potential target genes of miR-613. PDCD10 was chosen for further study along with genes that may be responsible for cell apoptosis. Bioinformatic analysis revealed that the 3'-UTR of PDCD10 contains a putative binding region of miR-613 (Figure 4A). To determine whether or not miR-613 directly targets PDCD10, an EGFP reporter analysis was performed. EGFP reporter vectors carrying the 3'-UTR of wild-type or mutant-type PDCD10 were transfected into H9c2 cells when miR-613 was over-expressed or inhibited. When miR-613 was overexpressed, the level of expression of the 3'-UTR of the wild-type decreased by almost 55%, while inhibition of miR-613 increased the the level of expression of the 3'-UTR of the wild-type by approximately 1.8-fold (Figure 4B). However, the level of expression of the 3'-UTR of the mutant-type was not affected by a change in miR-613 expression.

RT-qPCR and Western blot analysis suggested that the miR-613 mimic decreased the level of expression of PDCD10 mRNA and PDCD10 protein; when miR-

613 was inhibited, however, PDCD10 expression was up-regulated (Figure 4C and 4D). All of these findings indicated that miR-613 down-regulates PDCD10 expression by directly binding to its 3'-UTR.

3.5. *miR-613 affected I/R-induced cardiomyocyte apoptosis by regulating the PI3K/Akt signaling pathway*

PI3K/Akt is an intracellular signaling pathway that is associated with cardioprotection (*10*). To further explore whether or not miR-613 also protected cardiomyocytes from I/R-induced injury by regulating the PI3K/Akt pathway, the level of expression of marker proteins such as p-Akt, the level of expression of the pro-apoptotic proteins CHOP and p-JNK, and the level of expression of the anti-apoptotic protein Bcl-2 were detected. Results suggested that miR-613 reduced the level of CHOP expression by 42% and that of p-JNK by 52% while it
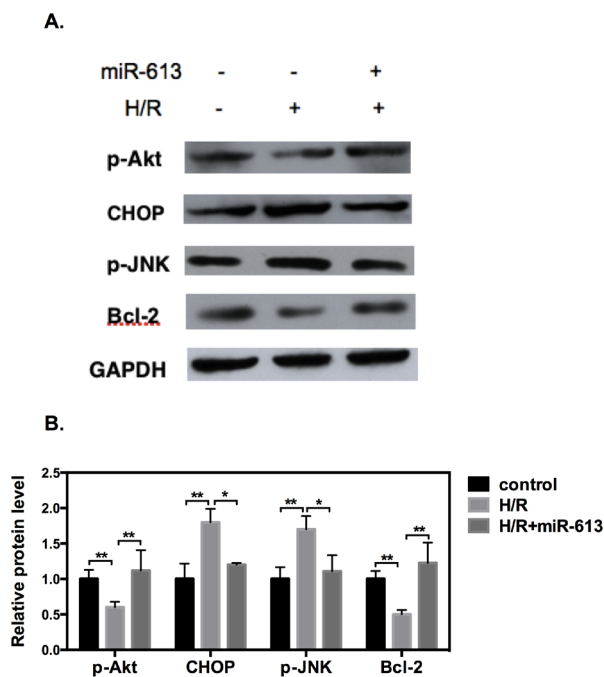

Figure 5. miR-613 suppressed I/R-induced cardiomyocyte apoptosis by regulating the PI3K/Akt signaling pathway. (A) Western blot analysis of the level of p-Akt, CHOP, p-JNK, and Bcl-2 proteins when an miR-613 mimic was transfected into H9c2 cells. **(B)** Statistical analysis of levels of protein expression. The histogram shows the mean ± S.D. of normalized GAPDH. *$p < 0.05$, **$p < 0.01$.
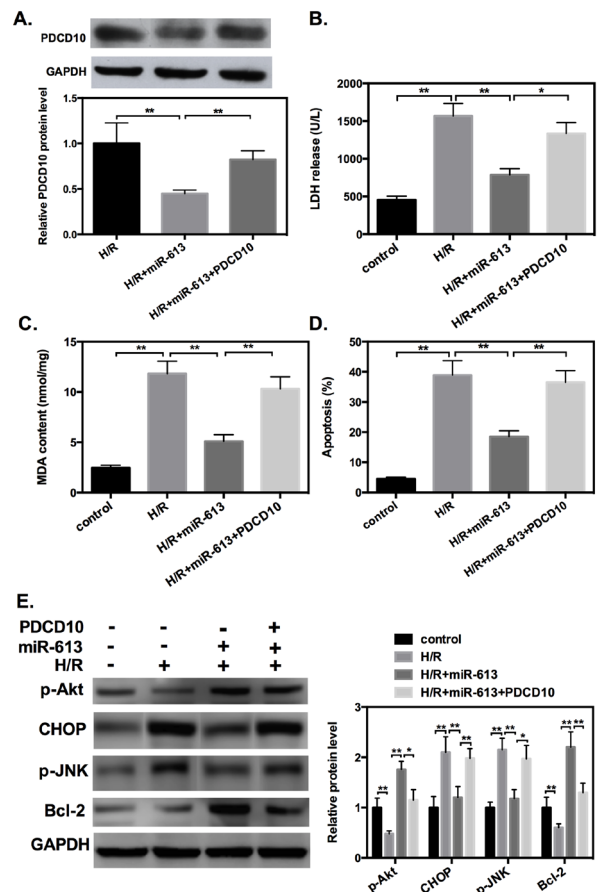
Figure 6. Restoration of PDCD10 counteracted the effect of miR-613 on the release of LDH, levels of MDA, and H/R-induced cardiomyocyte apoptosis. (A) Western blot analysis was performed to detect PDCD10 protein expression in h9c2 cells with or without restored PDCD10. **(B)** Ectopic expression of PDCD10 neutralized inhibition of the release of LDH by miR-613. **(C)** Ectopic expression of PDCD10 neutralized inhibition of MDA levels by miR-613. **(D)** Ectopic expression of PDCD10 counteracted inhibition of cardiomyocyte apoptosis by miR-613. **(E)** Restoration of PDCD10 counteracted the effect of miR-613 on the PI3K/Akt pathway. *$p < 0.05$, **$p < 0.01$.

increased the expression of p-Akt by 1.8-fold and the expression of Bcl-2 by 1.5-fold (Figure 5).

3.6. *miR-613 affected I/R-induced cardiomyocyte apoptosis by directly targeting PDCD10*

The data above indicate that miR-613 down-regulates the expression of PDCD10 at both the mRNA and protein levels. To further determine whether or not PDCD10 was the functional target gene, a rescue experiment was performed. miR-613 and a PDCD10 expression plasmid without the 3'-UTR were transfected into H9c2 cells, and results indicated that overexpression of PDCD10 neutralized the decrease in PDCD10 expression induced by miR-613 (Figure 6A). Restoration of PDCD10 counteracted the effect of miR-613 on the release of LDH, levels of MDA, H/R-induced cardiomyocyte apoptosis, and PI3K/Akt signaling pathways (Figure 6B-6D). These findings suggest that miR-613 acts on I/R-induced cell apoptosis by directly regulating PDCD10.

4. Discussion

Recent animal experiments and clinical studies have indicated that cell apoptosis is closely related to myocardial I/R-induced injury. Thus far, numerous miRNAs have been reported to be associated with myocardial I/R injury by regulating target genes, including miR-451, miR-133a, and Lin28a (*11-13*). The current study investigated the potential role of miR-613 in myocardial I/R injury and results indicated that the level of miR-613 expression decreased by 43% in H9c2 cells after H/R treatment in comparison to the level of expression in the controls. This finding suggests that miR-613 may play a role in I/R injury to cardiomyocytes.

The specific effects of miR-613 were determined. Results indicated that an miR-613 mimic decreased an H/R-induced increase in the release of LDH, levels of MDA, and cardiomyocyte apoptosis. Furthermore, several apoptosis-related proteins were significantly up-regulated as a result of H/R injury, but this increase was reversed by overexpression of miR-613. These findings indicate that miR-613 suppressed cardiomyocyte apoptosis and it protected cardiomyocytes from H/R-induced injury.

To further illustrate the molecular mechanism by which miR-613 functions, its target genes were predicted and eventually verified. PDCD10 is also known as cerebral cavernous malformation 3 (CCM3), and it plays an important role in regulating apoptosis, neoangiogenesis, and certain tumor signaling pathways (*14-16*). Mounting evidence indicates that PDCD10 plays a pivotal role in regulating cell survival and death. In different type of cells, PDCD10 is reported to be both pro-apoptotic (*17*) and anti-apoptotic (*18*), suggesting that apoptosis by PDCD10 is context-dependent.

Bioinformatic analyses suggested that PDCD10 is a potential target of miR-613. This prediction was confirmed by an EGFP reporter assay. Moreover, miR-613 down-regulated the expression of PDCD10 at both the mRNA and protein levels. A rescue experiment was performed to further explore whether or not PDCD10 is a target gene of miR-613. A PDCD10 expression plasmid without the 3'-UTR and an miR-613 mimic were co-transfected into H9c2 cells. Results showed that restoration of PDCD10 counteracted the effect of miR-613 on the release of LDH, levels of MDA, H/R-induced cardiomyocyte apoptosis. That is, miR-613 acts in I/R-induced cardiomyocyte apoptosis by directly targeting PDCD10.

The PI3K/Akt signaling pathway is a major signaling that promotes cell survival and proliferation (*19*). When PI3K is activated, it acquires the ability to phosphorylate PIP2 into PIP3 and leads to activation of Akt. Activated Akt then translocates from the cell membrane to the cytoplasm and nucleus and can activate or suppress many downstream proteins to regulate cellular functions (*20*). Phosphorylated PI3K/Akt inhibits pro-apoptotic substrates, such as CHOP and p-JNK, while it promotes the anti-apoptotic substrate Bcl-2 (*21*). Recent evidence suggests that PDCD10 is associated with the activation of Akt signaling protein (*22*). The current study found that miR-613 significantly increased the level of p-Akt and Bcl-2 expression; when miR-613 was overexpressed, however, the level of expression of the pro-apoptotic proteins CHOP and p-JNK decreased significantly. Furthermore, ectopic expression of PDCD10 restored the effect of miR-613 on the PI3K/Akt signaling pathway. These findings indicate that miR-613 can inhibit I/R-induced cardiomyocyte apoptosis by targeting PDCD10 by regulating PI3K/Akt signaling pathways.

Taken together, the current findings are the first to show that miR-613 can suppress I/R-induced cardiomyocyte apoptosis by down-regulating PDCD10 and activating PI3K/Akt pathways. PDCD10 is a direct target gene of miR-613. The current results reveal the molecular mechanism by which miR-613 affects I/R-mediated apoptosis, and this finding may help facilitate the treatment of myocardial I/R injury.

Acknowledgements

References

1.　Hu X, Zhou X, He B, Xu C, Wu L, Cui B, Wen H, Lu Z, Jiang H. Minocycline protects against myocardial ischemia and reperfusion injury by inhibiting high mobility group box 1 protein in rats. Eur J Pharmacol. 2010; 638:84-89.
2.　Thind GS, Agrawal PR, Hirsh B, Saravolatz L, Chen-Scarabelli C, Narula J, Scarabelli TM. Mechanisms

of myocardial ischemia-reperfusion injury and the cytoprotective role of minocycline: Scope and limitations. Future Cardiol. 2015; 11:61-76.

3. Ke ZK, Xu P, Shi Y, Gao AM. MicroRNA-93 inhibits ischemia-reperfusion induced cardiomyocyte apoptosis by targeting PTEN. Oncotarget. 2016; 7:28796-28805.

4. Song S, Seo HH, Lee SY, Lee CY, Lee J, Yoo KJ, Yoon C, Choi E, Hwang KC, Lee S. MicroRNA-17-mediated down-regulation of apoptotic protease activating factor 1 attenuates apoptosome formation and subsequent apoptosis of cardiomyobytes. Biochem Biophys Res Commun. 2015; 465:299-304.

5. Wang W, Zhang H, Wang L, Zhang S, Tang M. miR-613 inhibits the growth and invasiveness of human hepatocellular carcinoma *via* targeting DCLK1. Biochem Biophys Res Commun. 2016; 473:987-992.

6. Fu X, Cui Y, Yang S, Xu Y, Zhang Z. MicroRNA-613 inhibited ovarian cancer cell proliferation and invasion by regulating KRAS. Tumour Biol. 2016; 37:6477-6483.

7. Zhong D, Zhang Y, Zeng YJ, Gao M, Wu GZ, Hu CJ, Huang G, He FT. MicroRNA-613 represses lipogenesis in HepG2 cells by downregulating LXRα. Lipids Health Dis. 2013; 12:32.

8. Sacco J, Adeil K. MicroRNAs: Emerging roles in lipid and lipoprotein metabolism. Curr Opin Lipidol. 2012; 23:220-225.

9. Zhai C, Tang G, Peng L, Hu H, Qian G, Wang S, Yao J, Zhang X, Fang Y, Yang S, Zhang X. Inhibition of microRNA-1 attenuates hypoxia/re-oxygenation-induced apoptosis of cardiomyocytes by directly targeting Bcl-2 but not GADD45Beta. Am J Transl Res. 2015; 7:1952-1962.

10. Yao H, Han X, Han X. The cardioprotection of the insulin-mediated PI3K/Akt/mTOR signaling pathway. Am J Cardiovasc Drugs. 2014; 14:433-442.

11. Xie J, Hu X, Yi C, Hu G, Zhou X, Jiang H. MicroRNA-451 protects against cardiomyocyte anoxia/reoxygenation injury by inhibiting high mobility group box 1 expression. Mol Med Rep. 2016; 13:5335-5341.

12. Li S, Xiao FY, Shan PR, Su L, Chen DL, Ding JY, Wang ZQ. Overexpression of microRNA-133a inhibits ischemia-reperfusion-induced cardiomyocyte apoptosis by targeting DAPK2. J Hum Genet. 2015; 60:709-716.

13. Zhang M, Sun D, Li S, Pan X, Zhang X, Zhu D, Li C, Zhang R, Gao E, Wang H. Lin28a protects against cardiac

ischemia/reperfusion injury in diabetic mice through the insulin-PI3K-mTOR pathway. J Cell Mol Med. 2015; 19:1174-1182.

14. He Y, Zhang H, Yu L, Gunel M, Boggon TJ, Chen H, Min W. Stabilization of VEGFR2 signaling by cerebral cavernous malformation 3 is critical for vascular development. Sci Signal. 2010; 3:ra26.

15. Fidalgo M, Guerrero A, Fraile M, Iglesias C, Pombo CM, Zalvide J. Adaptor protein cerebral cavernous malformation 3 (CCM3) mediates phosphorylation of the cytoskeletal proteins ezrin/radixin/moesin by mammalian Ste20-4 to protect cells from oxidative stress. J Biol Chem. 2012; 287:11556-11565.

16. Aguirre AJ, Brennan C, Bailey G, Sinha R, Feng B, Leo C. Zhang Y, Zhang J, Gans JD, Bardeesy N, Cauwels C, Cordon-Cardo C, Redston MS, DePinho RA, Chin L. High-resolution characterization of the pancreatic adenocarcinoma genome. Proc Natl Acad Sci U S A. 2004; 101:9067-9072.

17. Schleider E, Stahl S, Wustehube J, Walter U, Fischer A, Felbor U. Evidence for anti-angiogenic and pro-survival functions of the cerebral cavernous malformation protein 3. Neurogenetics. 2011; 12:83-86.

18. Zhu Y, Wu Q, Xu JF, Miller D, Sandalcioglu IE, Zhang JM, Sure U. Differential angiogenesis function of CCM2 and CCM3 in cerebral cavernous malformations. Neurosurg Focus. 2010; 29:E1.

19. Shaw RJ, Cantley LC. Ras, PI(3)K and mTOR signalling controls tumor cell growth. Nature. 2006; 441:424-430.

20. Zhang J, Yu XH, Yan YG, Wang C, Wang WJ. PI3K/Akt signaling in osteosarcoma. Clin Chim Acta. 2015; 444:182-192.

21. Atif F, Yousuf S, Stein DG. Anti-tumor effects of progesterone in human glioblastoma multiform: Role of PI3K/Akt/mTOR signaling. J Steroid Biochem Molr Biol. 2015; 146:62-73.

22. Lambertz N, EI Hindy N, Kreitschmann-Andermahrl, Stein KP, Dammann P, Oezkan N, Mueller O, Sure U, Zhu Y. Downregulation of programmed cell death 10 is associated with tumor cell proliferation, hyperangiogenesis and peritumoral edema in human glioblastoma. BMC cancer. 2015, 15:759.